Quantum Theory of Bulk and Nanostructure Crystals

Quantum Theory of Bulk and Nanostructure Crystals

By

Rostam Moradian and Chinedu E. Ekuma

Cambridge
Scholars
Publishing

Quantum Theory of Bulk and Nanostructure Crystals

By Rostam Moradian and Chinedu E. Ekuma

This book first published 2024

Cambridge Scholars Publishing

Lady Stephenson Library, Newcastle upon Tyne, NE6 2PA, UK

British Library Cataloguing in Publication Data
A catalogue record for this book is available from the British Library

Copyright © 2024 by Rostam Moradian and Chinedu E. Ekuma

All rights for this book reserved. No part of this book may be reproduced, stored in a retrieval system, or transmitted, in any form or by any means, electronic, mechanical, photocopying, recording or otherwise, without the prior permission of the copyright owner.

ISBN (10): 1-0364-0212-6
ISBN (13): 978-1-0364-0212-9

Rostam Moradian: Dedicated to my family and the entire Lak community.

Chinedu Ekuma: To the roots that anchored me and the wings that lifted me to soar.

Contents

Preface

This book focuses on bulk and nanostructure crystals, and specifically discusses possible crystal lattices, their reciprocal lattices, and the Bragg relation for determining crystal structure. It describes band theory in independent electron approximation using the usual perturbation quantum theory, as well as how the internal electric field of the lattice periodic potential affects degenerate states at the Brillouin zone boundaries by using the Stark effect, which leads to energy bands separated by energy gaps. The book also discusses low-dimensional systems and nanostructures using the free electron model and tight binding model. The band structure and wave function of graphene, graphene nanoribbons, single-wall carbon nanotubes, and double-wall carbon nanotubes are obtained. Additionally, nanostructure vibrations are discussed.

Targeted at senior undergraduate and graduate students, alongside researchers with an interest in various topics within condensed matter physics, this text employs straightforward methodologies to introduce and clarify foundational concepts of crystal structure physics for undergraduates.

Rostam Moradian Razi university, Kermanshah, Iran
Chinedu Ekuma Lehigh University, USA

Chapter 1

Bulk and nano structures crystalography

A crystal is constructed by bringing its component atoms close enough together so that the nuclei of each atom interact with the electrons of neighboring atoms. Generally, for most systems, the total energy of a solid phase is lower than that of other phases, expressed as $E_{solid} < E_{gas\ or\ liquid}$. Figure 1.1 illustrates the construction of a solid phase.

Electrons in a solid usually divide into two parts: first, electrons which are strongly bonded to their atoms and hence cannot move, and second, electrons which can move throughout the solid. The nuclei of atoms plus static electrons are called the ion core, while the dynamic electrons are usually valance electrons. This is illustrated in Fig.1.2. Coulomb repulsion between ion cores, electron-ion core attraction, and electron-electron repulsion, along with the Pauli exclusion principle, are responsible for the construction of a solid. The ion cores prevent further compression of a solid due to the Pauli exclusion principle and Coulomb repulsion. Solids can be categorized into crystals and amorphous structures. A crystal has an ordered structure, whereas an amorphous solid lacks long-range order. This discussion focuses solely on crystal solids. Fig.1.3 (a) and (b) display two different crystal structures, where (a) all bases are symmetrically equivalent, while in (b) they are not. Fig.1.3 (c) depicts an amorphous structure schematically. The basis of a crystal could be an atom, multiple atoms, or a molecule. The lattice of a crystal is defined by replacing each basis with a mathematical point called a lattice site. Fig.1.4 demonstrates the construction of a crystal from a lattice and its basis.

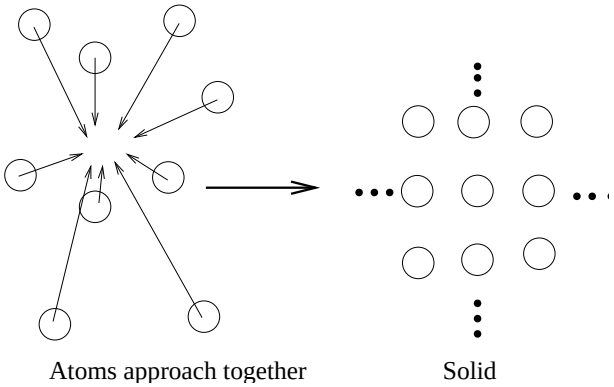

Figure 1.1: Illustration of the process of atoms approaching each other to construct a solid structure

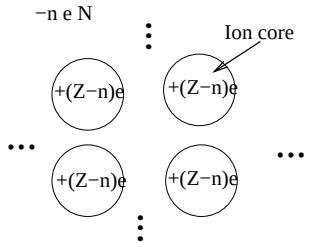

Figure 1.2: Illustration of valance electrons in a solid constructed from N atoms, where each atom has n valance electrons. The valance electrons charge of the solid is $-n\ e\ N$ and of the cores is $+(Z-n)eN$.

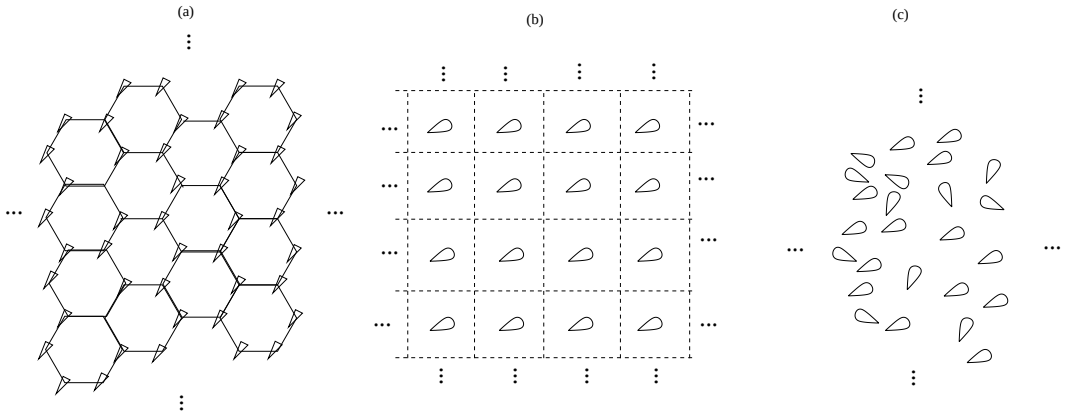

Figure 1.3: (a) and (b) depict two different crystal structures, and (c) shows an amorphous structure schematically.

Lattice sites can either be symmetrically equivalent or not. If the lattice sites are ordered and have equivalent symmetry, then the lattice is called a Bravais lattice. Fig.1.3 (a) shows a non-Bravais lattice, while (b) depicts a Bravais lattice. Non-Bravais lattices can often be converted to Bravais lattices by choosing proper lattice sites with multiple sub-sites. For example, the lattice in Fig.1.3 (a) can be converted to a Bravais lattice by selecting new lattice points at the midpoints between two sublattice points of the old lattice sites, as illustrated in Fig.1.5. Fig.1.6 shows two quasi one-dimensional and a three-dimensional non-Bravais lattices, where for (a) by choosing two sites as one Bravais site with two subsites and for (c) by considering four sites as one Bravais lattice site, they are converted to one-dimensional lattice sites.

To identify the positions of Bravais lattice points, we consider three primitive vectors, $\mathbf{a}_1$, $\mathbf{a}_2$, and $\mathbf{a}_3$. All

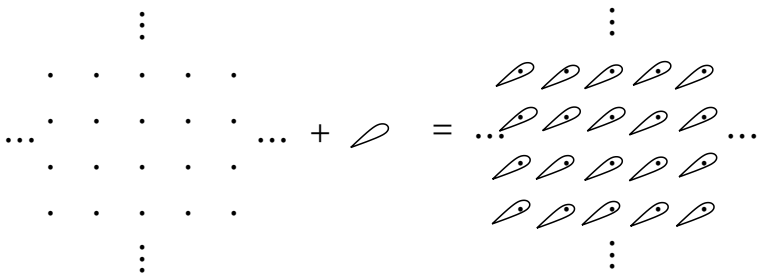

Figure 1.4: Demonstration of a crystal composed of a lattice and its basis.

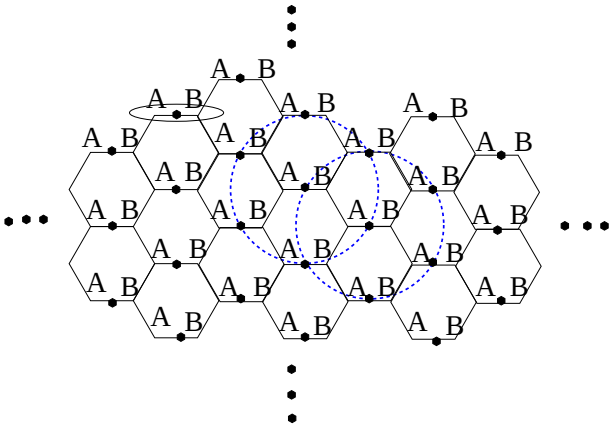

Figure 1.5: Conversion of a non-Bravais lattice to a Bravais lattice by selecting appropriate subsites.

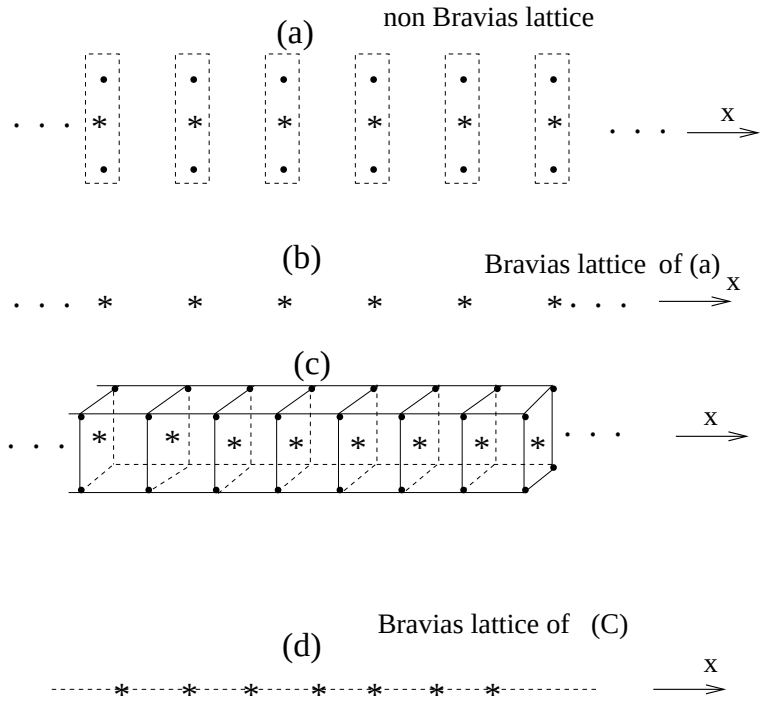

Figure 1.6: (a) and (c) depict two non-Bravais lattices, while (b) and (d) show their corresponding Bravais lattices. In (a), each Bravais lattice has two subsites, while in (c), each Bravais lattice has four subsites.

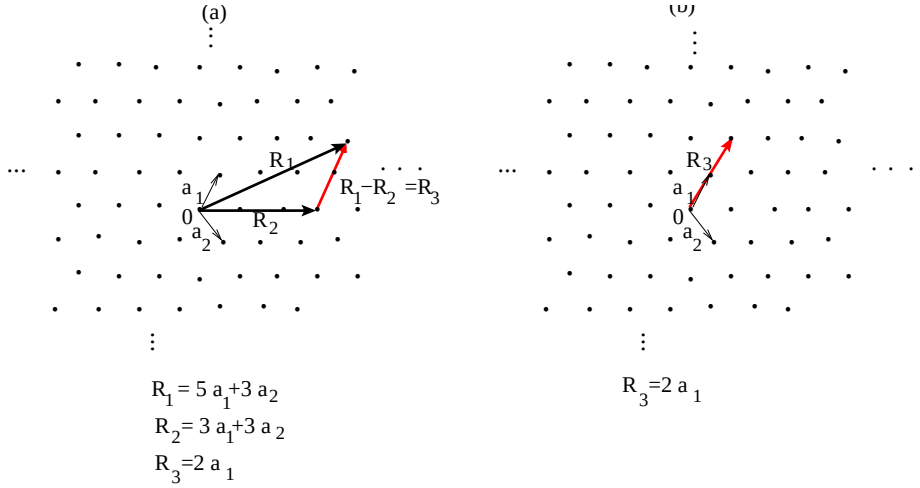

Figure 1.7: (a) Shows two different lattice point vectors $\mathbf{R}_1$ and $\mathbf{R}_2$ and their difference $\mathbf{R}_1 - \mathbf{R}_2 = \mathbf{R}_3$ in a two-dimensional hexagonal lattice. (b) Identifies a lattice point represented by $\mathbf{R}_3$.

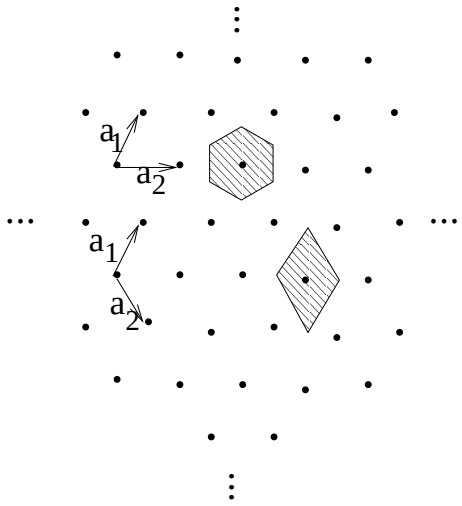

Figure 1.8: Illustrates two different unit cells of a two-dimensional hexagonal lattice.

lattice point vectors can be expressed as linear combinations of these primitive vectors with integer coefficients:

$$\mathbf{R}_{n_1,n_2,n_3} = \sum_{i=1}^{3} n_i \mathbf{a}_i \tag{1.1}$$

Given that lattice lengths are infinite, $n_1, n_2, n_3 = 0, \pm 1, \pm 2, \ldots$. Fig.1.7 illustrates a two-dimensional hexagonal Bravais lattice and the vectors representing the positions of two different points. It is important to note that the difference between any two of these vectors indicates the position of another point.

The symmetry of a lattice defines and limits all physical quantities such as the electron's band structure, X-ray diffraction patterns, electronic conductivity, among others. Calculating physical quantities for an infinite-dimensional Bravais lattice is challenging. However, since all lattice sites are equivalent and these quantities are periodic with respect to lattice sites, we can focus on a small volume of the lattice that includes one lattice site and retains all symmetries of the original lattice. In one, two, and three-dimensional lattices, the length, surface, or volume that includes one Bravais lattice site is known as a unit cell. Each unit cell is constructed from a set of vectors called primitive vectors. Fig.1.8 shows two sets of primitive vectors for a two-dimensional hexagonal lattice. For each Bravais lattice, there are many independent unit cells with different

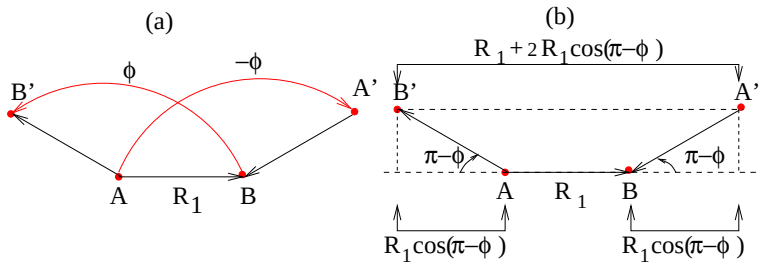

Figure 1.9: (a) and (b) Display two sites of a two-dimensional lattice located at points A and B. The vector $\mathbf{R}_1$ connects these two points. The $\mathbf{R}_1$ vector is rotated around the axis at A and B perpendicular to this system, resulting in the transition from A to A' and B to B'.

shapes, hence there are different possible sets of primitive vectors. It is possible to categorize Bravais lattices using possible group symmetries such as rotation, mirror, inversion center, and translation. In terms of these symmetries, there are fourteen distinct three-dimensional Bravais lattice systems, divided into seven categories. The parameters that specify each of these systems are the lengths of the crystal axes a, b, and c, and the angles between them, where the angle between b and c is α, between a and c is β, and between a and b is γ. For simplicity, in two-dimensional systems, all Bravais lattices can be derived by applying possible rotations consistent with translational invariance. The two-dimensional lattice site vectors with primitive vectors $\mathbf{a}_1$ and $\mathbf{a}_2$ are:

$$\mathbf{R}_{n_1,n_2} = \sum_{i=1}^{2} n_i \mathbf{a}_i \tag{1.2}$$

where the angle between $\mathbf{a}_1$ and $\mathbf{a}_2$ is γ. Consider a two-dimensional lattice that remains invariant under rotation ϕ around an axis perpendicular to the plane of the system. We examine two different ϕ rotations of the vector $\mathbf{R}_1$ that connects points A and B of this lattice. One rotation is anti-clockwise around an axis perpendicular to the lattice plane passing through point A, and the other is clockwise around another axis passing through B and perpendicular to the lattice plane. We denote the positions of rotated points A and B as A' and B', respectively. Since the entire lattice under these rotations returns to its original state, A' and B' should be lattice points. The vector connecting A' and B' has the same direction as $\mathbf{R}_1$ vector. Therefore, this vector should be an integer multiple of $\mathbf{R}_1$. Fig.1.9 (a) illustrates the beginning and end of the two-dimensional system's $\mathbf{R}_1$ primitive vector under ϕ and $-\phi$ rotations around an axis perpendicular to the two-dimensional system. Fig.1.9 (b) shows the difference between the rotated vectors in terms of the rotation angle and R_1 length. Since the lattice points should remain unchanged under these rotations, both A' and B' should be lattice points. Thus, the distance between them, $\mathbf{R}_{A'} - \mathbf{R}_{B'}$, should be a lattice vector parallel to $\mathbf{a}_1$, i.e., $\mathbf{R}_{A'} - \mathbf{R}_{B'} = p\,\mathbf{R}_1$, where p is an integer number to be determined. Consequently, we have:

$$|\mathbf{R}_{A'} - \mathbf{R}_{B'}| = R_1 - 2R_1 \cos\phi = p\, R_1 \Longrightarrow \cos\phi = \frac{1-p}{2} \tag{1.3}$$

Considering that $-1 \leq \cos\phi \leq 1$, it follows that:

$$-1 \leq \frac{1-p}{2} \leq 1 \implies -1 \leq p \leq 3 \tag{1.4}$$

We now identify the two-dimensional Bravais lattices corresponding to each p value in Eq.1.4. Starting with $p = 1$, this implies $B'A' = 1\mathbf{R}_1$ and $\cos\phi = 0$, corresponding to a rotation angle $\phi = \frac{\pi}{2}$. For simplicity, let $\mathbf{R}_1 = \mathbf{a}_1$. Fig.1.10 shows these rotations and the possible lattice that returns to itself under those rotations.

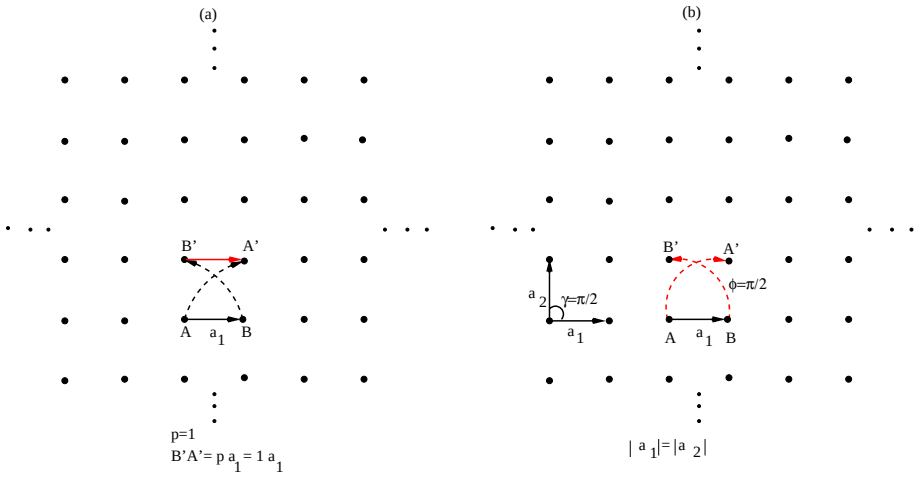

Figure 1.10: (a) Shows the lattice points A' and B' as the rotated points of A and B such that $B'A' = \mathbf{a}_1$. This configuration is possible only for a square lattice with equal lengths of primitive vectors $|\mathbf{a}_1| = |\mathbf{a}_2|$ and an angle between them, γ, of $\frac{\pi}{2}$, as presented in (b).

(a) Points A and B are two lattice points connected by $\mathbf{a}_1$. $B'A' = 1\mathbf{a}_1$. The lattice with $p = 1$ is a square lattice with primitive vectors $\mathbf{a}_1$ and $\mathbf{a}_2$ where $|\mathbf{a}_2| = |\mathbf{a}_1|$ and the angle between them, γ, is $\frac{\pi}{2}$.

For $p = 0$, as illustrated in Fig.1.11 (a) and (b), the system forms a hexagonal lattice with a rotation angle of $\phi = \frac{\pi}{3}$. The primitive vectors $\mathbf{a}_1$ and $\mathbf{a}_2$ are of equal magnitude ($|\mathbf{a}_2| = |\mathbf{a}_1|$) and the angle between them, denoted as γ, is $\frac{\pi}{3}$. For $p = 2$, with $BA = \mathbf{a}_1$ and $B'A' = 2\mathbf{a}_1$, as shown in Fig.1.11 (c) and (d), the system remains a hexagonal lattice but with a rotation angle of $\phi = \frac{2\pi}{3}$. Here, the primitive vectors $\mathbf{a}_1$ and $\mathbf{a}_2$ are again equal in length, and the angle γ between them remains $\frac{\pi}{3}$.

For $p = 3$, as illustrated in Fig.1.12, the system transforms into a rectangular lattice with a rotation angle of $\phi = \pi$, differing lengths of primitive vectors ($|\mathbf{a}_1| \neq |\mathbf{a}_2|$), and an angle γ between its axes of $\frac{\pi}{2}$.

The last structure corresponds to $p = -1$, where $B'A' = -AB$. As illustrated in Fig.1.13, the rotation angle is $\phi = 2\pi$, and the primitive vectors differ in length ($|\mathbf{a}_1| \neq |\mathbf{a}_2|$). This structure is known as oblique.

The possible rotation angles are illustrated in Table 1.1.

Table 1.1: Table showing the possible rotation angles for two-dimensional lattices, with corresponding rotation fold values.

p	ϕ	$n = \lvert\frac{2\pi}{\phi}\rvert$
3	$\pm\pi$	2
2	$\pm\frac{2\pi}{3}$	3
1	$\pm\frac{\pi}{2}$	4
0	$\pm\frac{\pi}{3}$	6
-1	$\pm 2\pi$	1

where $n = \frac{2\pi}{\phi}$ is known as the rotation fold. For $n = 4$, the preservation of lattice sites after rotation necessitates that the primitive vectors and the angle between them conform to

$$a_2 = a_1, \quad \gamma = \frac{\pi}{2}. \tag{1.5}$$

Fig.1.14 (a) and (b) demonstrate a square lattice and its $\frac{\pi}{2}$ rotation, respectively. As shown in Fig. 1.15, this

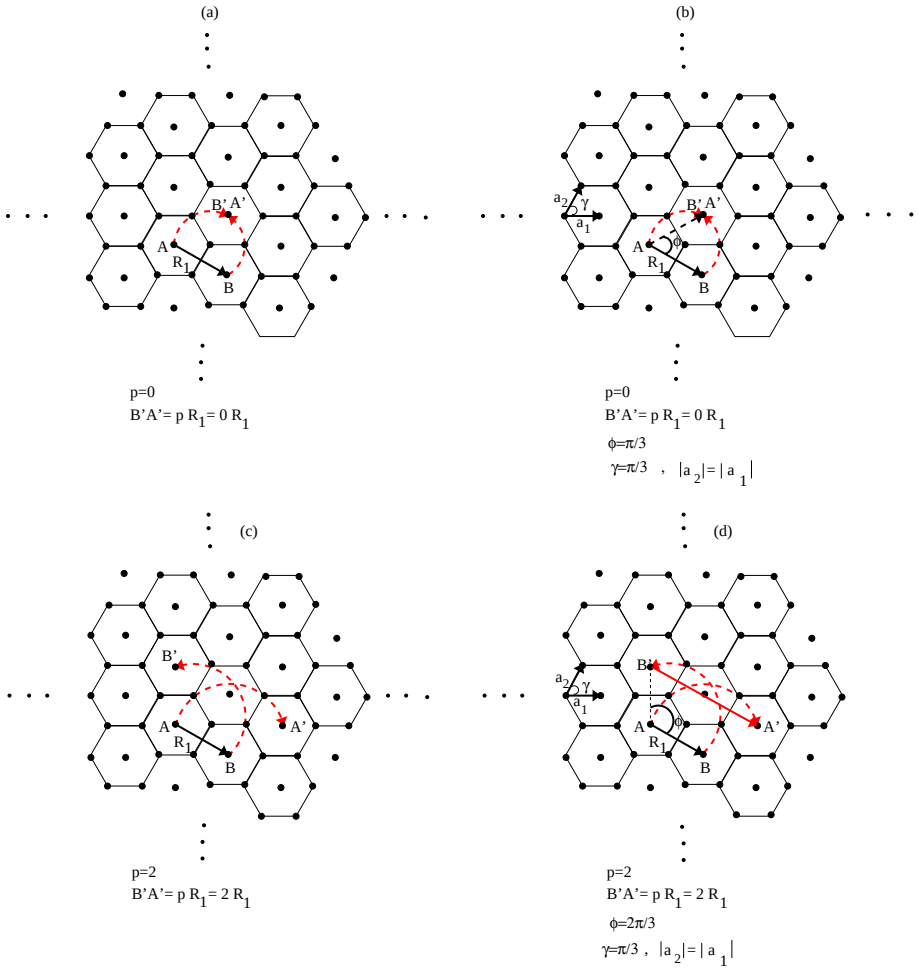

Figure 1.11: Illustrating the hexagonal lattice for $p = 0$ and $p = 2$. For $p = 0$, as seen in (a) and (b), the lattice is formed with rotation angle $\phi = \frac{\pi}{3}$ and equal primitive vectors. For $p = 2$, depicted in (c) and (d), the lattice maintains its hexagonal structure but with a rotation angle $\phi = \frac{2\pi}{3}$.

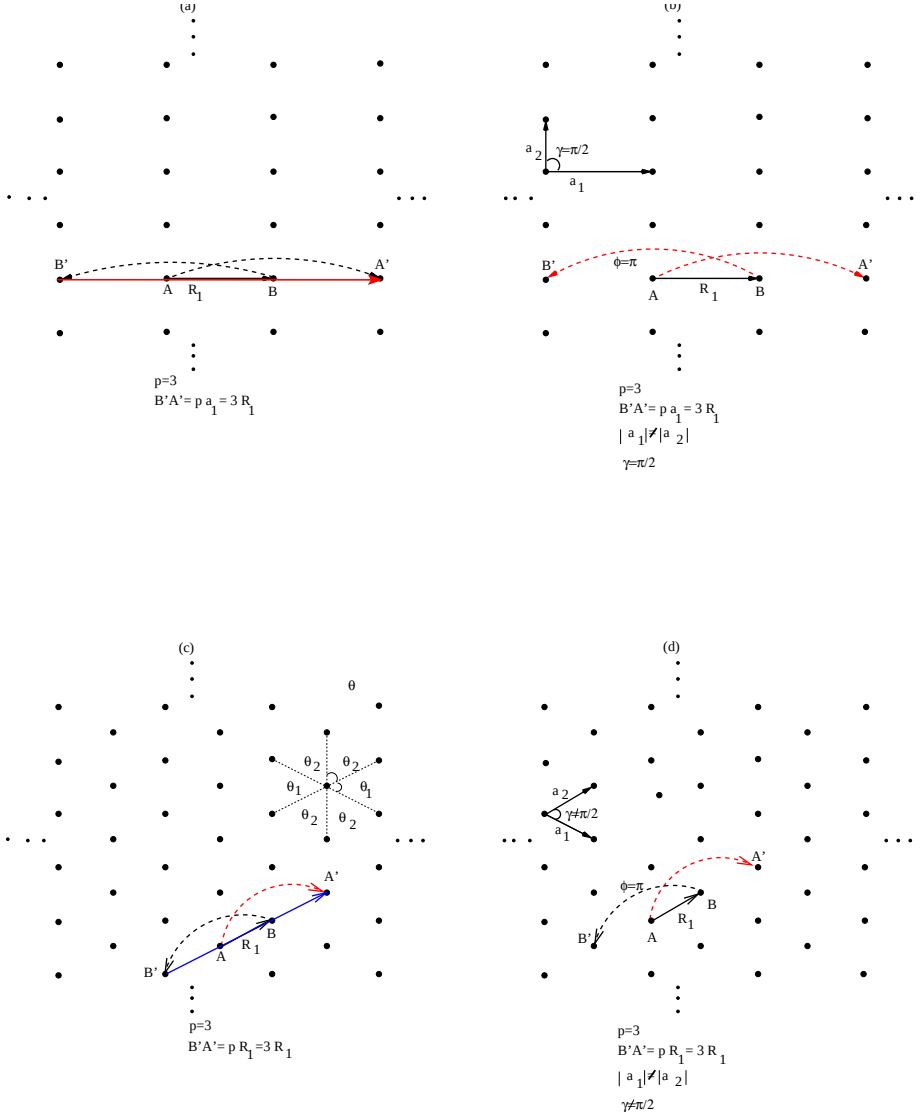

Figure 1.12: Depicting a rectangular lattice for $p = 3$. Panels (a) and (b) show the lattice with a rotation angle of $\phi = \pi$. Panels (c) and (d) illustrate a centered rectangular lattice, also with a rotation angle of $\phi = \pi$, but with non-equal angular measures $\theta_2 \neq \theta_1$ and $\theta_2, \theta_1 \neq \frac{\pi}{2}$.

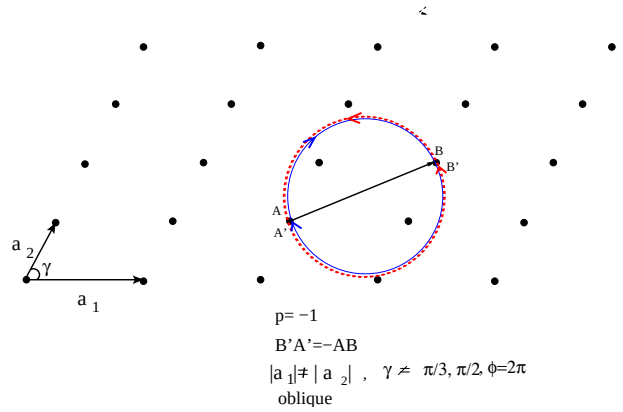

Figure 1.13: Presenting the oblique structure for $p = -1$ with $B'A' = -AB$. This structure features a rotation angle of $\phi = 2\pi$, an angle γ that is neither $\frac{\pi}{3}$ nor $\frac{\pi}{2}$, and non-equal lengths of the primitive vectors.

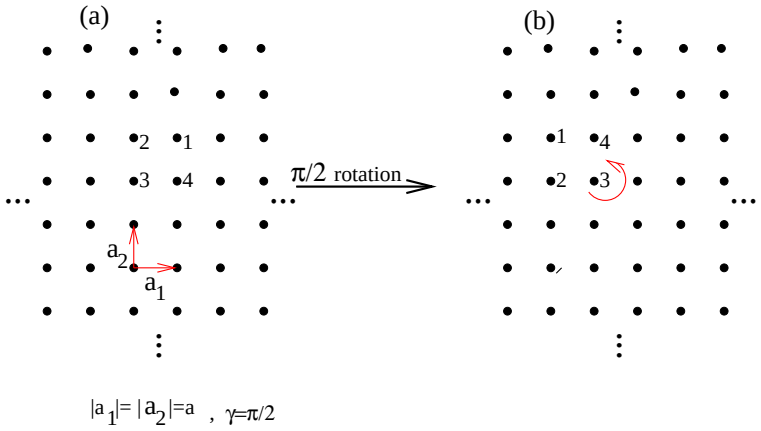

Figure 1.14: (a) and (b) depict a square lattice, illustrating that a $\frac{\pi}{2}$ rotation leaves the lattice unchanged.

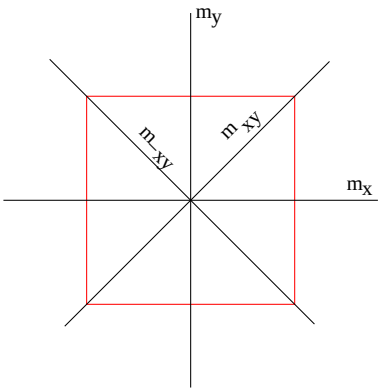

Figure 1.15: This figure illustrates the reflection mirrors of a square lattice, highlighting that the rotation axis is perpendicular to the lattice and intersects the square's center.

system possesses four mirror reflections at $y = 0$ (m_x), $x = 0$ (m_y), $y = x(m_{xy})$, and $y = -x$ (m_{-xy}) that maintain the original lattice structure. These mirrors run parallel to the rotation axis, which is perpendicular to the square surface and intersects its center. The symmetry of this lattice is denoted by $4m_xm_y = 4mm$, with the angle between mirrors being $\frac{2\pi}{4} = \frac{\pi}{2}$. For $n = 2$ with a rotation angle of $\frac{\pi}{2}$, the primitive vectors should differ in length $(a_2 \neq a_1)$, but $\gamma = \frac{\pi}{2}$. This lattice has perpendicular mirrors intersecting at the rectangular center, as depicted in Fig.1.16. For $n = 3$ or $n = 6$, the only viable configuration is $a_2 = a_1$ with $\gamma = \frac{\pi}{3}$ or $\gamma = \frac{2\pi}{3}$, as shown in the following figure. Another possibility for $n = 2$ is the centered rectangular or rhombic lattice, where $a_2 \neq a_1$ and $\gamma \neq \frac{\pi}{2}, \frac{\pi}{3}$, and $\frac{2\pi}{3}$. This lattice is illustrated in the next figure. The final structure,

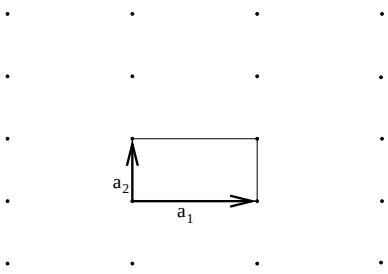

Figure 1.16: This figure shows a rectangular lattice with differing primitive vector lengths $(a_2 \neq a_1)$ and an angle $\gamma = \frac{\pi}{2}$.

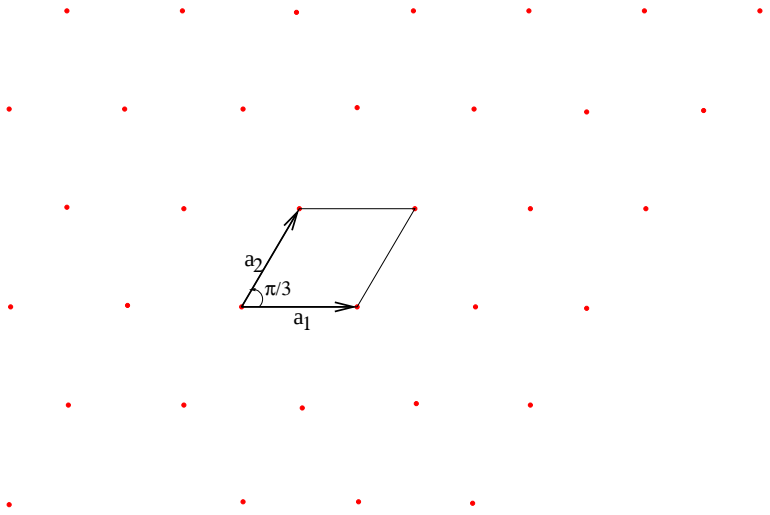

Figure 1.17: This figure presents a hexagonal two-dimensional lattice with equal primitive vectors ($|\mathbf{a}_1| = |\mathbf{a}_2| = a_1$) and angles of $\gamma = \frac{\pi}{3}$ or $\frac{2\pi}{3}$.

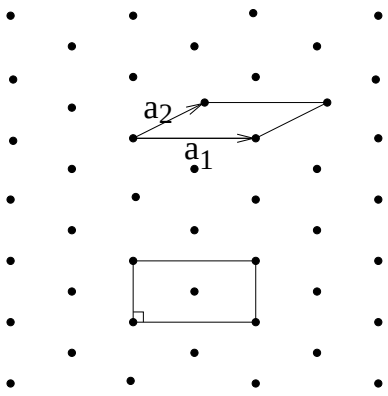

Figure 1.18: This figure illustrates the unit cell and centered rectangular cell of the rhombic two-dimensional lattice, where $a_1 \neq a_2$.

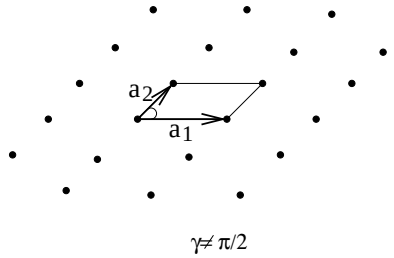

Figure 1.19: This figure displays the unit cell of the oblique two-dimensional lattice, where $a_1 \neq a_2$ and $\gamma \neq \frac{\pi}{2}$.

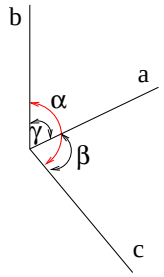

Figure 1.20: Illustration of the crystal axes and the angles between them.

for $n = 1$, is known as oblique, characterized by $a_1 \neq a_2$ and $\gamma \neq \frac{\pi}{2}$, as depicted in the figure below. Table 1.2 outlines the allowed two-dimensional Bravais lattices and their parameters.

Table 1.2: Table summarizing the allowed two-dimensional Bravais lattices and their corresponding parameters.

n (rotation fold order)	γ	a_2	lattice name	symmetry
2	$\frac{\pi}{2}$	$\neq a_1$	rectangular, centered rectangular	2mm
3	$\frac{2\pi}{3}$	$= a_1$	hexagonal	6mm
4	$\frac{\pi}{2}$	$= a_1$	square	4mm
6	$\frac{\pi}{3}$	$= a_1$	hexagonal	6mm
1	$\neq \frac{\pi}{3}, \frac{2\pi}{3}, \frac{\pi}{2}$	$\neq a_1$	oblique	1

A three-dimensional lattice is defined by three axes and the angles between them, with its primitive vectors denoted as $\mathbf{a}_1$, $\mathbf{a}_2$, and $\mathbf{a}_3$ along the a, b, and c axes, respectively. Fig.1.20 illustrates the crystal axes and the angles between them: α is the angle between the b and c axes, β is the angle between the a and c axes, and γ is the angle between the a and b axes. To determine all possible three-dimensional Bravais lattices, two-dimensional lattices are rotated around three crystal axes. The first rotation angle, ϕ_1, must align with one of the permissible angles for two-dimensional Bravais lattices: $\phi_1 = \frac{\pi}{3}, \frac{\pi}{2}, \pi, \frac{2\pi}{3}, 2\pi$. The other two rotation angles around the remaining independent axes are $\phi_2 = \frac{\pi}{3}, \frac{\pi}{2}, \pi, \frac{2\pi}{3}, 2\pi$ and $\phi_3 = \frac{\pi}{3}, \frac{\pi}{2}, \pi, \frac{2\pi}{3}, 2\pi$. Different combinations of $\{\phi_1, \phi_2, \phi_3\}$ or their corresponding rotation folds $n_j = \frac{2\pi}{\phi_j}$ are considered, such that the combination of these three rotations returns the crystal to its original orientation. Additionally, other symmetries like mirror (indicated by m) or inverse center (indicated by a minus sign, $-$) are taken into account. As with a two-dimensional Bravais lattice, rotations by $\frac{\pi}{3}$ and $\frac{2\pi}{3}$ lead to the same hexagonal lattice with $|\mathbf{a}_1| = |\mathbf{a}_2|$ or $b = a$. This means that a rotation of $\frac{2\pi}{3}$ aligns the primitive vector $\mathbf{a}_1$ with $\mathbf{a}_2$ around the c-axis, perpendicular to the $\mathbf{a}_1 - \mathbf{a}_2$ plane. For $\phi_1 = \frac{\pi}{3}$, only rotations of $\phi_2 = \pi$ and $\phi_3 = \pi$ around the two other axes return the lattice sites to one another, as depicted in Fig.1.21, characterizing a hexagonal

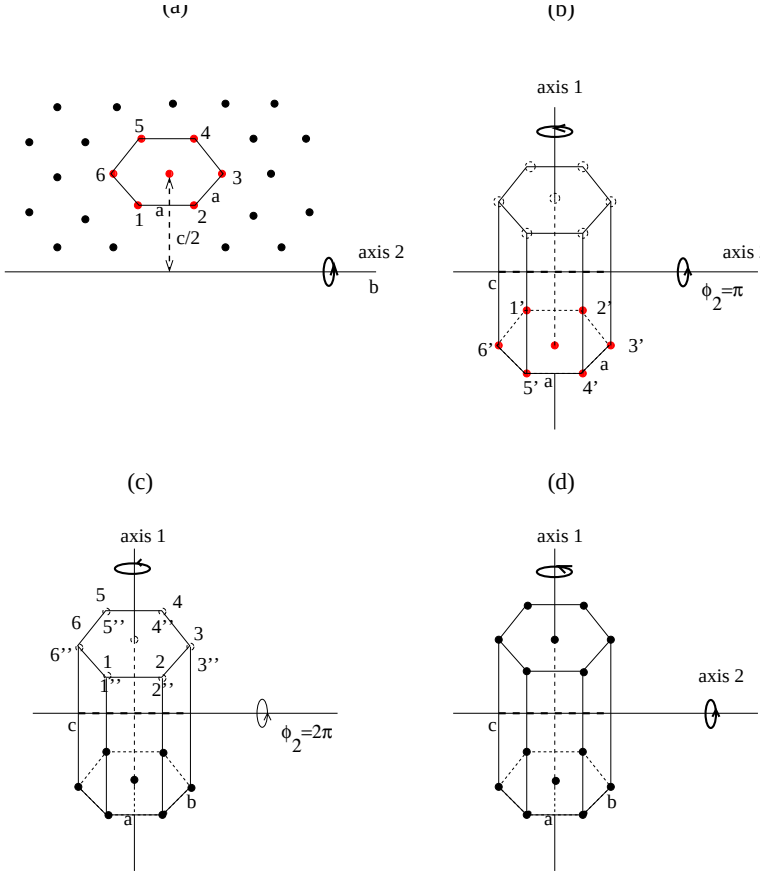

Figure 1.21: (a) Demonstrates that rotation by $\phi_1 = \frac{\pi}{3}$ around axis 1 returns the two-dimensional hexagon to itself, as does rotation by $\phi_2 = \pi$ or $\phi_3 = \pi$ around axes 2 and 3. (b) Shows that rotations by $\phi_1 = \frac{\pi}{3}$ or $\phi_1 = \frac{2\pi}{3}$ around axis 1 return the three-dimensional hexagon to itself, but only rotations by π around axes 2 and 3 yield the same result.

lattice. Considering the rotation of two-dimensional square lattices, how many three-dimensional lattices can be obtained? All possible structures should be considered. Initially, consider a square lattice placed $\frac{a}{2}$ apart from a rotation axis parallel to the lattice, as shown in Fig. 1.22 (a). Sequential rotations by $\phi_2 = \frac{\pi}{2}$ around axis 2 or a single rotation by $\phi_2 = \frac{\pi}{2}$ around axis 2 followed by sequential rotations by $\phi_1 = \frac{\pi}{2}$ around axis 1 yield a three-dimensional simple cubic (SC) lattice. In Fig.1.22 (a), if rotation axis 2 is located at $\frac{c}{2}$ away from the square lattice, as illustrated in Fig.1.23 (a), rotations by $\phi_2 = \pi$ and sequential $\phi_1 = \frac{\pi}{2}$ yield a simple tetragonal lattice, as shown. Another structure comprises two parallel square lattices spaced $z = \frac{c}{2}$ apart, with the second lattice shifted by $\frac{1}{2}\mathbf{a}_1$ and $\frac{1}{2}\mathbf{a}_2$ in the $\mathbf{a}_1$ and $\mathbf{a}_2$ directions. Sequential rotations by $\phi_2 = \frac{\pi}{2}$ around axis 2 or by $\phi_1 = \frac{\pi}{2}$ around axis 1 yield a body-centered tetragonal lattice, as depicted in Fig.1.24. In Fig.1.24, if the distance between the two square lattices equals $\frac{a}{2}$, subsequent rotations by $\phi_2 = \frac{\pi}{2}$ around axis 2 create a body-centered cubic lattice (BCC), as illustrated in Fig.1.25.

The last cubic structure is obtained sequentially from $\phi_2 = \frac{\pi}{2}$ rotations of two square lattices, one of which is shifted by $\frac{1}{2}\mathbf{a}_1$ and $\frac{1}{2}\mathbf{a}_2$ in the $\mathbf{a}_1$ and $\mathbf{a}_2$ directions, as illustrated in Fig.1.26.

For rotation $\phi_1 = \pi$ around axis 1, there are four possible structures that are invariant under this rotation: rectangular, centered rectangular, body rectangular, and face center rectangular, as illustrated in Fig.1.27 (a), (b), (c), and (d). Rotation by $\phi_2 = \pi$ or $\phi_3 = \pi$ around 2 and 3 axes returns lattice sites to themselves. Fig.1.27 (e), (f), (g), and (h) show these four different lattices, which are called simple, base center, body

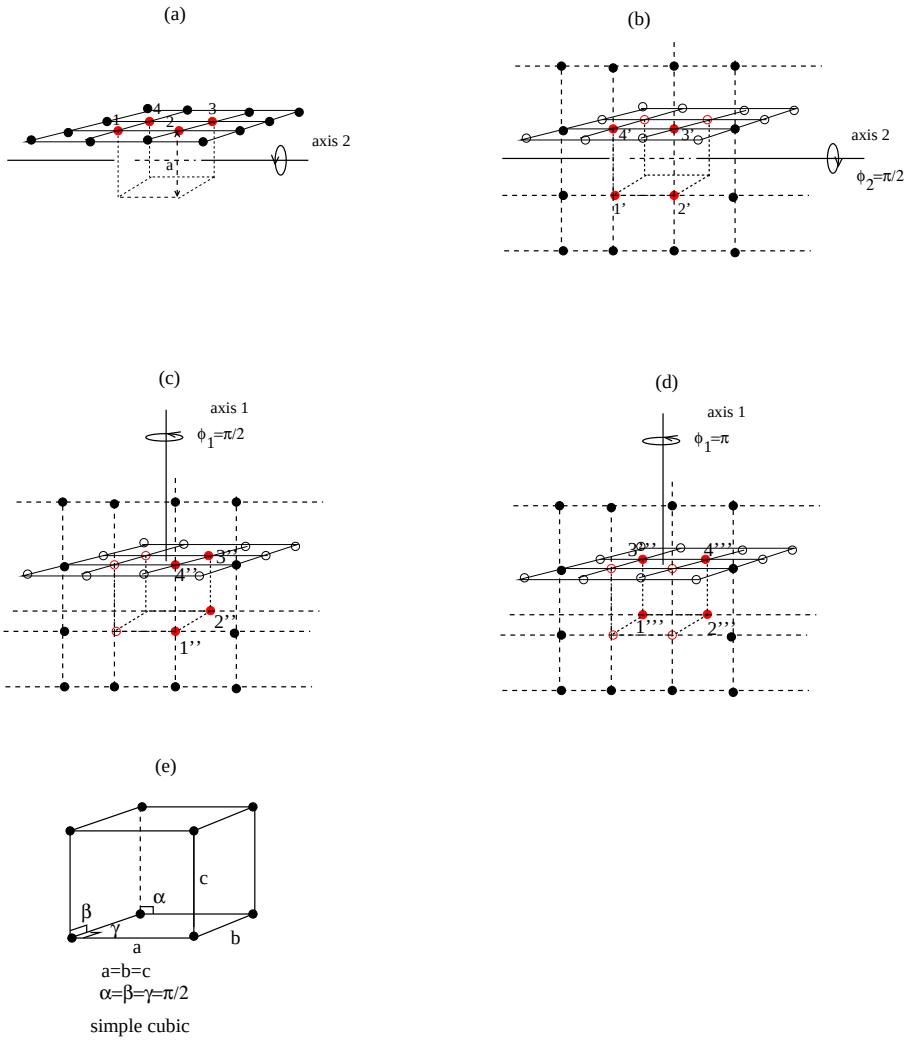

Figure 1.22: (a) Illustrates that rotation by $\phi_2 = \frac{\pi}{2}$ around axis 2 transforms a two-dimensional square lattice into a vertical square two-dimensional lattice (b). Three such rotations return the lattice to its original state. (c) and (d) show the rotated lattice in (b) further rotated by $\phi_1 = \frac{\pi}{2}$ around axis 1 sequentially to return to its original state. (e) Illustrates the simple cubic (SC) lattice.

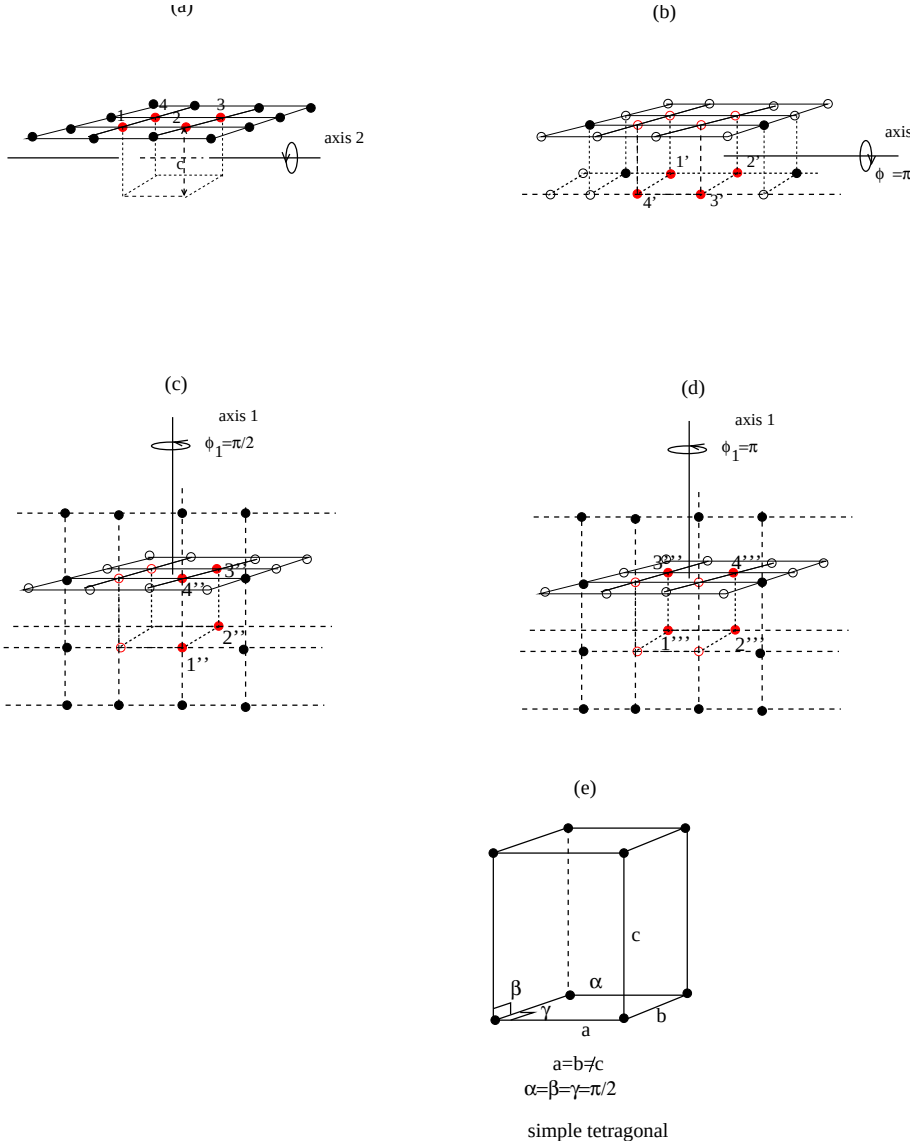

Figure 1.23: (a) Shows a square two-dimensional lattice. (b) Illustrates that the square two-dimensional lattice in (a), rotated by $\phi_2 = \pi$ around axis 2 at $z = \frac{c}{2}$, converts to a horizontal square two-dimensional lattice at $z = c$. Sequential π rotations return the lattice to its original state. Another method involves sequential $\frac{\pi}{2}$ rotations of the rotating square two-dimensional lattice in (a) around axis 1.

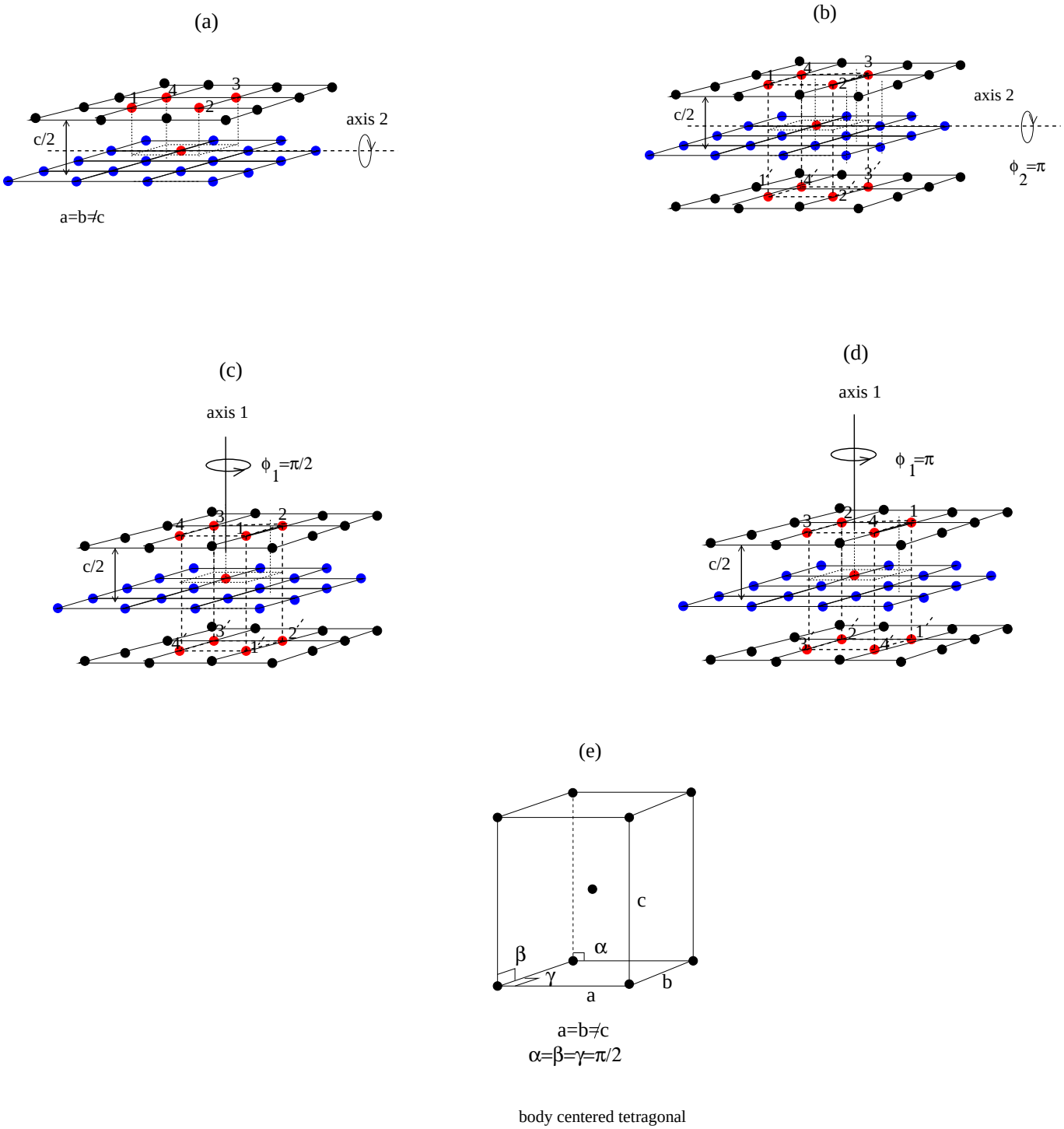

Figure 1.24: (a) Shows two square lattices spaced $\frac{c}{2}$ apart. (b) Illustrates the system in (a) rotated under $\phi_2 = \pi$ around axis 2. Another $\phi_2 = \pi$ rotation returns it to its original state. An alternative method involves sequential $\phi_1 = \frac{\pi}{2}$ rotations of the system in (b) around axis 1, as shown in (c) and (d).

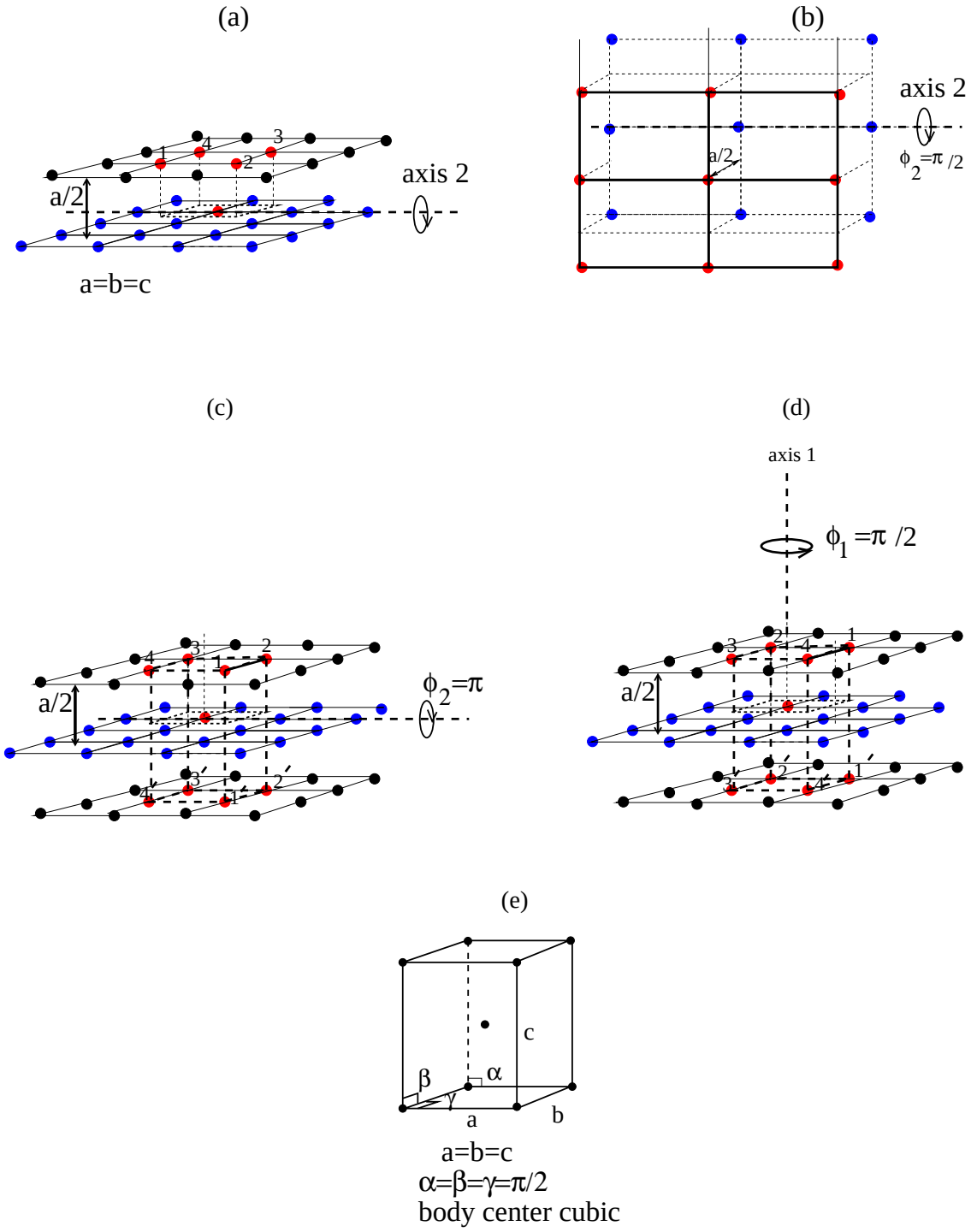

Figure 1.25: (a) Shows two square lattices spaced $\frac{a}{2}$ apart. (b) Illustrates the system in (a) rotated under $\phi_2 = \pi$ around axis 2. Another $\phi_2 = \pi$ rotation returns it to its original state. An alternative method involves sequential $\phi_1 = \frac{\pi}{2}$ rotations of the system in (b) around axis 1, as shown in (c) and (d).

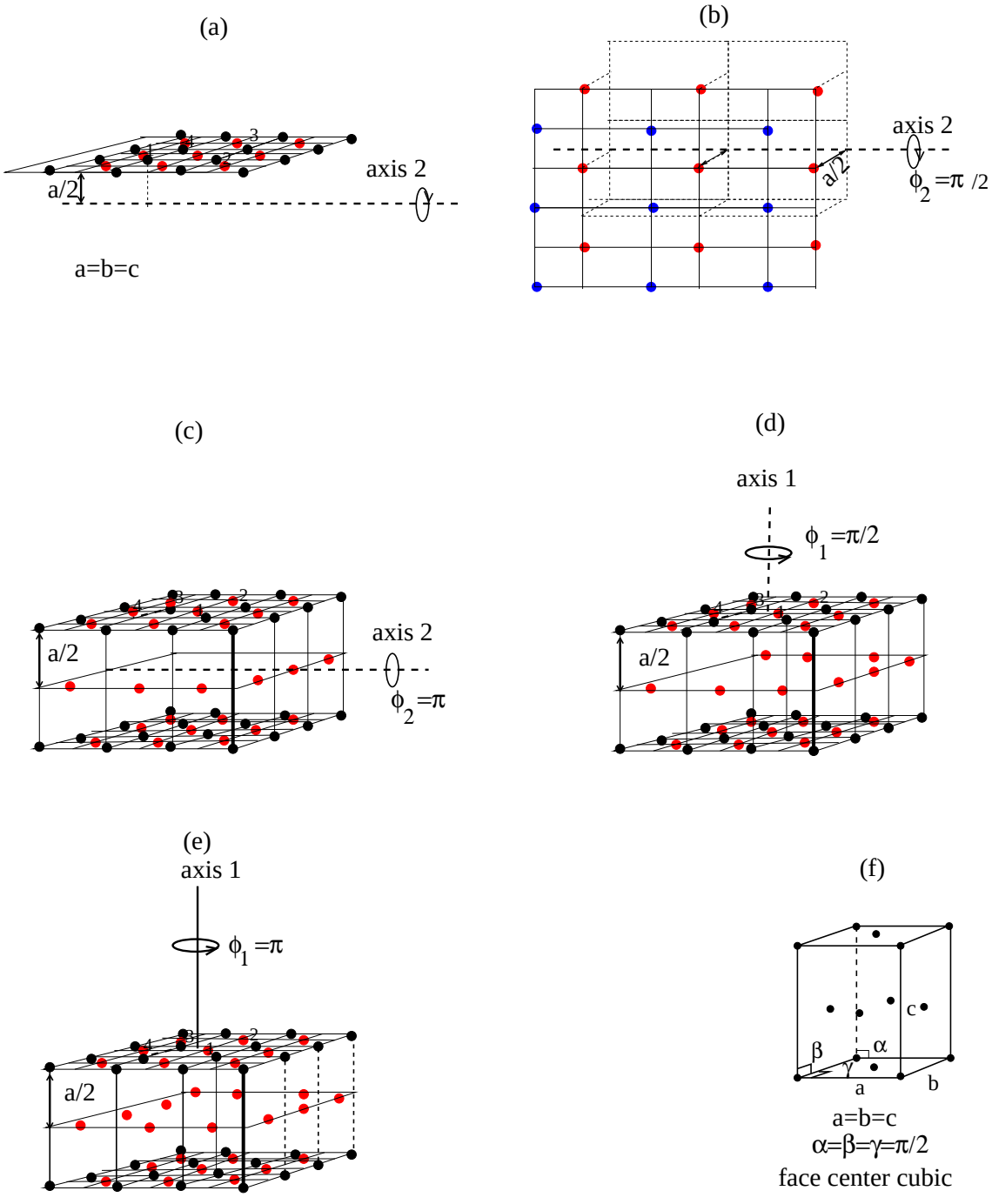

Figure 1.26: (a) shows two square lattices spaced by $\frac{a}{2}$ apart. (b) illustrates the system in (a) rotated by $\phi_2 = \pi$ around axis number 2. By another $\phi_2 = \pi$ rotation, it returns to itself. Another way is sequential $\phi_1 = \frac{\pi}{2}$ rotations of the system in (b) around the 1-axis, as illustrated in (c) and (d).

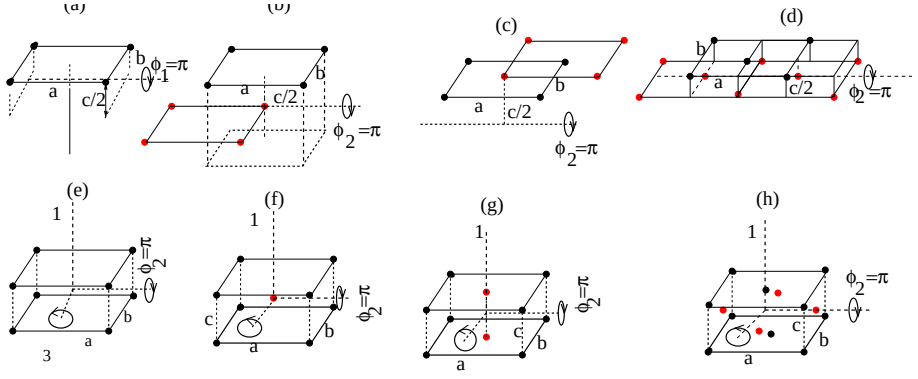

Figure 1.27: (a) illustrates a two-dimensional simple rectangular lattice. By rotation $\phi_2 = \pi$ around axis 2, we have a simple rectangular orthorhombic lattice as shown in (e). (b) shows two rectangular lattices spaced apart by $\frac{c}{2}$. By rotating them by $\phi_2 = \pi$ around axis 2, we obtain a body center rectangular orthorhombic lattice as shown in (f). For the centered rectangular lattice, rotation by $\phi_2 = \pi$ around axis 2, with $\frac{c}{2}$ distance from the lattice in (c), results in a base-centered rectangular orthorhombic lattice as shown in (g). Two centered rectangular lattices, each $\frac{c}{2}$ apart from the other, rotate by $\phi_2 = \pi$ around the 2-axis. The obtained lattice is the face center rectangular orthorhombic lattice shown in (h).

center, and face center orthorhombic lattices, respectively.

One of the possible three-dimensional lattices is obtained from an oblique lattice by rotating $\phi_3 = \pi$ around the 3rd axis, which is $\frac{a}{2}$ apart from the oblique lattice, as illustrated in Fig.1.28 (a), (b), and (c). In (b), $\{1', 2', 3', 4'\}$ are rotated versions of $\{1, 2, 3, 4\}$ by $\phi = \pi$ around axis 3. This is called a simple monoclinic lattice. Another one is obtained from (d) where two parallel obliques are shifted by $a/2$. In (e), $\{1', 2', 3', 4'\}$ are rotated versions of $\{1, 2, 3, 4\}$ by $\phi = \pi$ around axis 3. (f) shows a base-center monoclinic lattice.

The last three-dimensional Bravais lattice obtained from an oblique lattice with no symmetry is triclinic.

Fig.1.29 shows possible Bravais lattices.

Note that an n-fold rotation axis with a mirror perpendicular to this axis is denoted by $\frac{n}{m}$.

By fixing the origin on one of the lattice sites, each Bravais lattice site's position can be written as a linear combination of primitive vectors,

$$\mathbf{R}_{n_1,n_2,n_3} = \sum_{i=1}^{3} n_i \mathbf{a}_i \tag{1.6}$$

where n_1, n_2, and n_3 are integer numbers that take all plus and minus numbers. Note that the volumes of all different-shaped unit cells of a Bravais lattice are equal. This can be proved as follows. Let us define the lattice number density of a lattice site with volume V and total lattice number N by

$$\rho = \frac{N}{V}. \tag{1.7}$$

Consider two unit cells with different shapes of a Bravais lattice with volumes V_1 and V_2, respectively. Since both unit cells include one lattice site, $N_1 = 1$ and $N_2 = 1$. Hence

$$\begin{aligned} V_1 &= \frac{N_1}{\rho} = \frac{1}{\rho} \\ V_2 &= \frac{N_2}{\rho} = \frac{1}{\rho} \end{aligned} \tag{1.8}$$

Eq.1.8 leads to the equality of unit cell volumes,

$$V_1 = V_2. \tag{1.9}$$

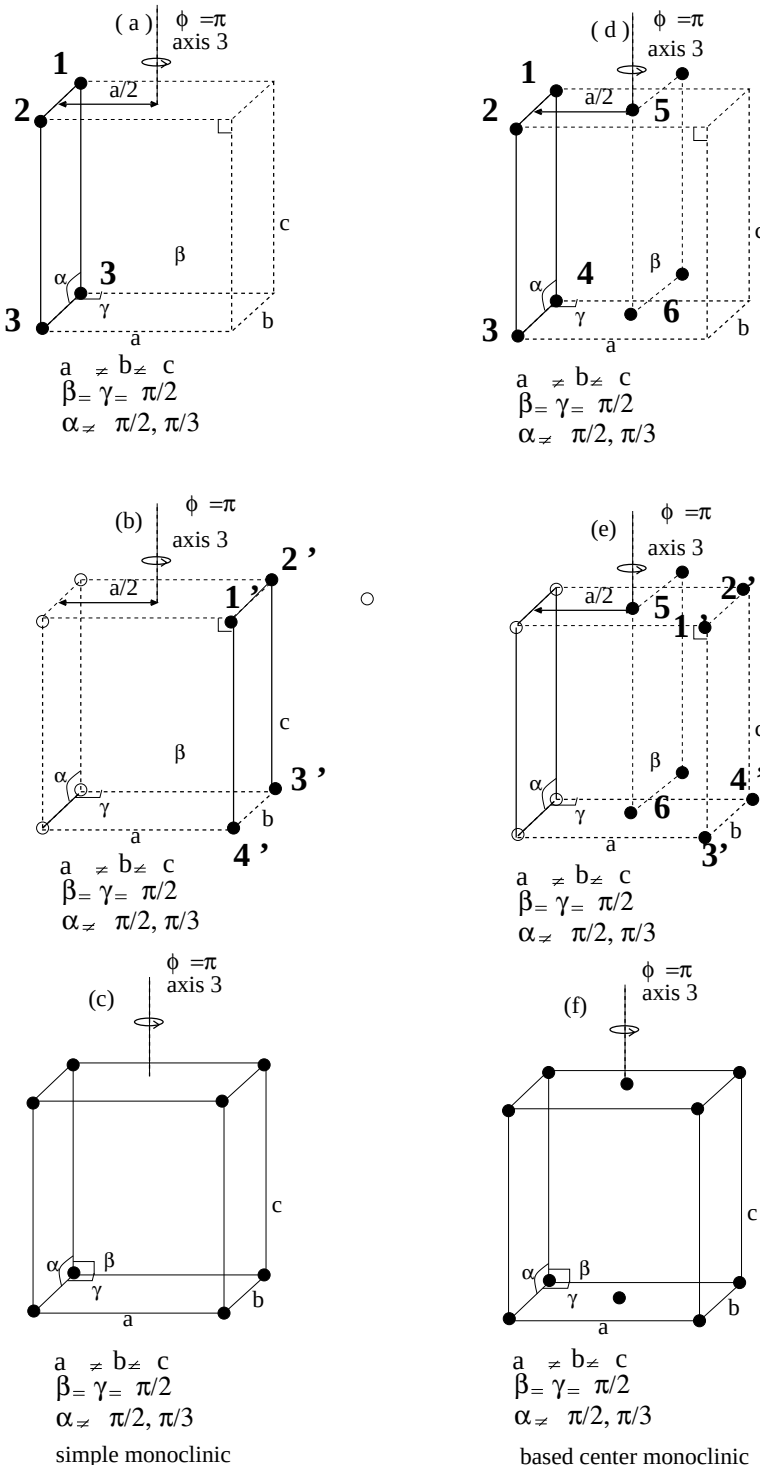

Figure 1.28: (a) illustrates an oblique lattice. (b) this lattice is rotated by π around axis number 3, which is $a/2$ apart from this lattice. (c) is an extra π rotation of (b) around axis 3, which is known as a simple monoclinic lattice. (d) shows two oblique lattices $a/2$ apart from each other. (e) shows rotation of (d) around axis 3 by π. One more π rotation around axis 3 returns it to (a). This is called a base-center monoclinic lattice.